Molecular Biology of the Cell
Vol. 17, 448–459, January 2006

Different Plk1 Functions Show Distinct Dependencies on Polo-Box Domain-mediated Targeting

Anja Hanisch, Anja Wehner, Erich A. Nigg, and Herman H.W. Silljé

Department of Cell Biology, Max Planck Institute for Biochemistry, D-82152 Martinsried, Germany

Submitted August 25, 2005; Revised October 14, 2005; Accepted October 24, 2005
Monitoring Editor: Ted Salmon

Polo-like kinase 1 (Plk1) has multiple important functions during M-phase progression. In addition to a catalytic domain, Plk1 possesses a phosphopeptide-binding motif, the polo-box domain (PBD), which is required for proper localization. Here, we have explored the importance of correct Plk1 subcellular targeting for its mitotic functions. We either displaced endogenous Plk1 through overexpression of the PBD or introduced the catalytic domain of Plk1, lacking the PBD, into Plk1-depleted cells. Both treatments resulted in remarkably similar phenotypes, which were distinct from the Plk1 depletion phenotype. Cells depleted of Plk1 mostly arrested with monoastral spindles, because of inhibition of centrosome maturation and separation. In contrast, these functions were not impaired in cells with mislocalized Plk1. Instead, these latter cells showed a checkpoint-dependent mitotic arrest characterized by impaired chromosome congression. Thus, whereas chromosome congression requires localized Plk1 activity, other investigated Plk1 functions are less dependent on correct PBD-mediated targeting. This opens the possibility that PBD-directed drugs might be developed to selectively interfere with a subset of Plk1 functions.

INTRODUCTION

Reversible protein phosphorylation by protein kinases and phosphatases plays a key role in the regulation of mitotic progression (Nigg, 2001; Vagnarelli and Earnshaw, 2004). Prominent among the mitotic kinases is Polo-like kinase 1 (Plk1) (Barr *et al*., 2004; Glover, 2005). Antibody microinjection and RNA interference (RNAi) studies have revealed functions for human Plk1 in centrosome maturation and spindle assembly (Lane and Nigg, 1996; Liu and Erikson, 2002; Sumara *et al*., 2004; van Vugt *et al*., 2004b). In the absence of Plk1, cells do not form a bipolar spindle and arrest in a prometaphase-like state with an activated mitotic spindle checkpoint (Sumara *et al*., 2004; van Vugt *et al*., 2004b). In addition, Plk1 has been implicated in chromatid arm separation through cohesin removal, which in vertebrate cells occurs during early mitosis (Sumara *et al*., 2002; Gimenez-Abian *et al*., 2004; Hauf *et al*., 2005). Later during M phase, Plk1 has been implicated in mitotic exit and cytokinesis (Carmena *et al*., 1998; Descombes and Nigg, 1998; Seong *et al*., 2002; Lindon and Pines, 2004; Lee *et al*., 2005). Roles in other processes, notably responses and adaption to DNA damage, have also been attributed to Polo kinases (Toczyski *et al*., 1997; Smits *et al*., 2000; van Vugt *et al*., 2004a).

In line with this multitude of proposed functions, vertebrate Plk1 localizes to diverse mitotic structures, including centrosomes, kinetochores, and the central spindle and midbody (Golsteyn *et al*., 1995; Lee *et al*., 1995; Arnaud *et al*., 1998; Barr *et al*., 2004). These localizations are mediated by the noncatalytic C-terminal half of Plk1 (Seong *et al*., 2002). This part of the kinase contains the so-called polo-box domain (PBD) that comprises two polo box motifs (Elia *et al*., 2003a). These constitute specific signatures of the Polo-like kinase family and have not been found in any other proteins. Using a phosphopeptide-based proteomic screen, Yaffe and coworkers discovered that the PBD constitutes a phosphopeptide-binding domain, which binds with maximal affinity to phosphopeptides containing a consensus sequence S-pS/pT-P/X (Elia *et al*., 2003a). Similar interactions were demonstrated for the PBDs of Polo kinases from other organisms as well as for the PBDs of human Plk2 and Plk3 (Elia *et al*., 2003b). Plk2 and Plk3 are structurally similar to human Plk1 but believed to function in distinct cellular processes (Barr *et al*., 2004).

Because the PBD of Plk1 interacted with a number of proteins only when these were phosphorylated at specific sites (Lowery *et al*., 2005), a model has been proposed according to which the Plk1 PBD docks to particular target proteins after phosphorylation by appropriate "priming" kinases (Elia *et al*., 2003a). Crystallography studies have confirmed specific binding of phosphopeptides to an interface formed by the two polo-box repeats (Cheng *et al*., 2003; Elia *et al*., 2003b). Two residues in human Plk1, His538 and Lys540, interact directly with the phosphate group of the peptide and are essential for phosphopeptide binding (Elia *et al*., 2003b). In addition to its purported targeting function, the PBD was also shown to interact with the catalytic domain of Plk1, resulting in a mutual inhibition of function, at least in vitro (Jang *et al*., 2002a). Interestingly, this interaction did not require a functional PBD phosphopeptide-binding motif, indicating that the catalytic domain interacts with the PBD through a different mechanism (Elia *et al*., 2003b). This notwithstanding, phosphopeptide binding to the PBD results in kinase activation, suggesting that the induction of a structural change liberates the catalytic domain from its inhibitory interaction with the PBD (Elia *et al*., 2003b). Similar to structurally related kinases, Plk1 activity is also regulated by phosphorylation of a residue (Thr210) within the so-called activation loop (Jang *et al*., 2002b). This phosphor-

This article was published online ahead of print in *MBC in Press* (http://www.molbiolcell.org/cgi/doi/10.1091/mbc.E05–08–0801) on November 2, 2005.

Address correspondence to: Herman H.W. Silljé (sillje@biochem.mpg.de).

Abbreviations used: PBD, polo-box domain.

ylation presumably stabilizes the activation loop in an open conformation, and, in addition, it prevents the binding of the PBD (Jang *et al*., 2002a). This may explain why the overexpression of PBD did not interfere with endogenous Plk1 kinase activity in vivo (Seong *et al*., 2002).

Ectopic expression of Plk1 in NIH 3T3 cells was reported to cause malignant transformation and tumor growth in nude mice (Smith *et al*., 1997). Moreover, aberrant expression of human Plk1 in tissue culture cells caused defects in both mitosis and cytokinesis (Mundt *et al*., 1997). Conceptually, this might lead to aneuploidy, a hallmark of most human tumors, and it is interesting, therefore, that many human cancers show elevated levels of Plk1 (Eckerdt *et al*., 2005; Takai *et al*., 2005). These observations suggest that Plk1 could constitute an attractive target for anticancer therapeutics and a first small molecule inhibitor of Plk1 has recently been described (Gumireddy *et al*., 2005). In this context, it is interesting to consider that inhibition of Plk1 function might be accomplished not only through targeting of the catalytic domain but also through interference with the PBD (Lowery *et al*., 2005).

In the present study, we have asked to what extent different Plk1 functions depend on PBD-mediated localization of Plk1. Specifically, we have explored the consequences of overexpression of PBD and compared the resulting mitotic arrest phenotypes with those seen after RNAi-mediated depletion of the kinase. We found that general catalytic activity of Plk1 was sufficient to bring about centrosome maturation, centrosome separation, and spindle assembly, but complete chromosome congression and continued progression through M phase were dependent on correctly localized Plk1 activity. These findings have implications for both our understanding of Plk1 function and the design of anti-Plk1 drugs.

MATERIALS AND METHODS

Cloning Procedures

The Plk1-PBD^{WT} (aa 326–603) was cloned in-frame by PCR into a pcDNA3.1 vector encoding a amino-terminal 3xmyc-tag (Invitrogen, Carlsbad, CA) using primers 5′-CCG GAA TTC CAG ATC TTC GAT TGC TCC CAG CAG CCT GG-3′ and 5′-CCG CTC GAG TTA GGA GGC CTT GAG ACG GTT GC-3′. The myc-tagged Plk2-PBD (aa 355–685) and Plk3-PBD (aa 336–646) constructs were PCR cloned in the same vector with the primers 5′-GGC GGA TCC CAC TTA TCA AGC CCA GCT AAG-3′ and 5′-GGC CTC GAG TCA GTT ACA TCT TTG TAA GAG C-3′ for PBD 2 and 5′-GGC GGA TCC CCC CCC AAC CCA GCT AGG AGT C-3′ and 5′-GGC CTC GAG CTA GGC TGG GCT GCG GTC CCG G-3′ for PBD3. The Plk1-PBD^{AA} mutant (H538A, K540A) was made by site-directed mutagenesis using the following primers: 5′-CAA TTC TCC GGA GCC CCG CCT ATC TGT CCC-3′ and 5′-GGG ACA GAT AGG CGG GGC TCC GGA GAA TTG-3′.

For generating the stable cell lines, the myc-tagged Plk1-PBD^{WT} and Plk1-PBD^{AA} gene fragments were introduced into the pcDNA4/TO vector (Invitrogen), in which the neomycin resistance marker had been replaced by a puromycin cassette.

For rescue experiments, an established Plk1-RNAi targeting sequence (Kraft *et al*., 2003) was cloned into the pTER+ vector (Brummelkamp *et al*., 2002; van de Wetering *et al*., 2003). RNAi resistant myc-tagged Plk1 constructs in the pcDNA3.1/3xmyc-C vector were generated by introducing six silent point mutations in the RNAi targeting sequence using primers 5′-TAA TGA ACT TCT GAA CGA TGA GTT CTT TAC TTC TGG CTA TAT C-3′ and 5′-ACT CAT CGT TCA GAA GTT CAT TAA TGG TTG GGC GGG CAG TGG G-3′. The catalytically impaired Plk1 contains the a K82R replacement and the Plk1 catalytic domain plasmid encodes amino acids 1–352. All PCR fragments and mutations were checked by sequencing.

Cell Culture and Generation of Inducible Stable Cell Lines

HeLa S3 cells were grown at 37°C under 5% CO_2 in DMEM (Invitrogen), supplemented with 10% fetal calf serum and penicillin-streptomycin (100 IU/ml and 100 μg/ml, respectively). For the generation of tetracycline-inducible cell lines, the plasmids encoding myc-tagged Plk1-PBD^{WT} and Plk1-PBD^{AA}, respectively, were transfected into a HeLa S3 cell line, which stably expressed a tet repressor gene under control of the cytomegalovirus promoter, together with a blasticidine resistance marker (pcDNA6/TR; Invitrogen). Stably transfected cell lines were established by selection with 5 μg/ml blasticidin and 1 μg/ml puromycin. The expression of myc-PBD^{WT} and myc-PBD^{AA} was induced by addition of 0.1 μg/ml tetracycline.

Transient Transfections and RNAi

Plasmid transfections were performed using FuGENE6 reagent (Roche Diagnostics, Indianapolis, IN) according to the manufacturer's instructions. Plk1, Nuf2, and Mad2 were depleted using small interfering RNA (siRNA) duplex oligonucleotides (Dharmacon Technologies, Lafayette, CO) targeting published sequences (DeLuca *et al*., 2002; Martin-Lluesma *et al*., 2002; Kraft *et al*., 2003). As a control, a duplex (GL2) targeting luciferase was used (Elbashir *et al*., 2001). siRNA duplexes were transfected using Oligofectamine (Invitrogen) as described previously (Elbashir *et al*., 2001). For rescue experiments, the Plk1-RNAi plasmid (or the empty pTER+ vector as a control) was transfected simultaneously with the respective myc-tagged Plk1 constructs (or myc-hWW45 as a control), and cells were fixed and analyzed 40 h later.

Immunofluorescence Microscopy

Cells were grown on coverslips and either fixed and permeabilized in −20°C methanol for 10 min or in 20 mM PIPES, pH 6.8, 4% formaldehyde, 0.2% Triton X-100, 10 mM EGTA, and 1 mM $MgCl_2$ for 10 min at room temperature. Afterward cells were incubated for 30 min at room temperature in blocking solution (phosphate-buffered saline [PBS], 1% bovine serum albumin). All antibody incubations were carried out for 1 h at room temperature in a humidified chamber, followed by three washes in PBS. Primary antibodies used in this study were mouse monoclonal antibody (mAb) anti-myc (1:10; 9E10 tissue culture supernatant), mouse mAb anti-α-tubulin-fluorescein isothiocyanate (1:1000; Santa Cruz Biotechnology, Santa Cruz, CA), rabbit anti-Plk1 (1 μg/ml; Abcam, Cambridge, United Kingdom), human ANA and CREST autoimmunsera (1:1000, Europa Bioproducts, Cambridge, United Kingdom; and 1:5000, Immunovision, Springdale, AR, respectively), mouse mAb anti-γ-tubulin (1:1000, GTU-88; Sigma-Aldrich, St. Louis, MO), rabbit anti-pericentrin (1:1000; Abcam), rabbit anti-centrin (1:600) and mouse mAb anti-centrin (20H5, 1:5000; gift from J. L. Salisbury, Mayo Clinic College of Medicine, Rochester, NY), mouse mAb anti-Aurora-A (1:1000; BD Biosciences PharMingen, San Diego, CA), mouse mAb anti-Hec1 (1:1000; Abcam) and rabbit anti-Mad2 serum (1:1000; Covance, Berkeley, CA). Primary antibodies were detected with Alexa Fluor 488- and Alexa Fluor 555-conjugated goat anti-mouse or anti-rabbit IgGs (1:1000; Invitrogen), respectively. DNA was stained with 4′,6-diamidino-2-phenylindole (DAPI; 2 μg/ml). Immunofluorescence microscopy was performed using a Zeiss Axioplan II microscope (Carl Zeiss, Jena, Germany) with Apochromat 40× and 63× oil immersion objectives, respectively. Photographs were taken using a Micromax charge-coupled device (CCD) camera (model CCD-1300-Y; Princeton Instruments, Trenton, NJ) and MetaView software (Visitron Systems, Puchheim, Germany). For high-resolution images, a Deltavision microscope on a Nikon Eclipse TE200 base (Applied Precision, Issaquah, WA) equipped with S Fluor 40×/1.3 and Plan Apo 60×/1.4 oil immersion objectives and a photometrics CoolSnap HQ camera was used for collecting 0.15-μm distanced optical sections in the z-axis. Images at single focal planes were processed with a deconvolution algorithm and then projected into one picture using the Softworx software (Applied Precision). Images were cropped in Adobe Photoshop 6.0 and then sized and placed in figures using Adobe Illustrator 10 (Adobe Systems, Mountain View, CA).

Cell Extracts and Western Blot Analysis

Cells were washed once with ice-cold PBS containing 1 mM phenylmethylsulfonyl fluoride, scraped off the plate, and resuspended in ice-cold HEPES lysis buffer (50 mM HEPES, pH 7.4, 150 mM NaCl, and 0.5% Triton X-100) containing 1 mM DTT, 30 μg/ml RNase A, 30 μg/ml DNase, protease, and phosphatase inhibitors. After 15 min on ice, lysed cells were centrifuged at 13,000 rpm for 15 min at 4°C. Protein concentrations in the cleared lysate were determined using the D_c protein assay (Bio-Rad, Hercules, CA), and equal protein amounts were loaded on SDS-PAGE gels. Separated proteins were transferred to nitrocellulose membranes (Whatman Schleicher and Schuell, Keene, NH). For Western blot analysis, mouse mAb anti-Plk1 (1:10, PL2, tissue culture supernatant), mouse mAb anti-α-tubulin (1:1000; Sigma-Aldrich), and mouse mAb anti-myc (1:10, 9E10, tissue culture supernatant) were used and detected by ECL Supersignal (Pierce Chemical, Rockford, IL) using a digital Fujifilm LAS-1000 camera attached to an Intelligent darkbox II (Raytest, Straubenhardt, Germany). For quantification of the signals, the Advanced Data Image Analyzer imaging software was used (Raytest).

Mitotic Chromosome Spreads

HeLa S3 cells were either treated with Plk1 siRNA oligonucleotides for 36 h or with nocodazole (100 ng/ml) overnight. The myc-PBD^{WT} stable cell line was induced for 24 h. Mitotic cells were collected by mitotic shake off, centrifuged for 4 min at 1000 rpm, and resuspended in diluted DMEM culture medium (40% DMEM without antibiotics and 60% deionized H_2O). The cells were allowed to swell at room temperature for 5 min before spinning and

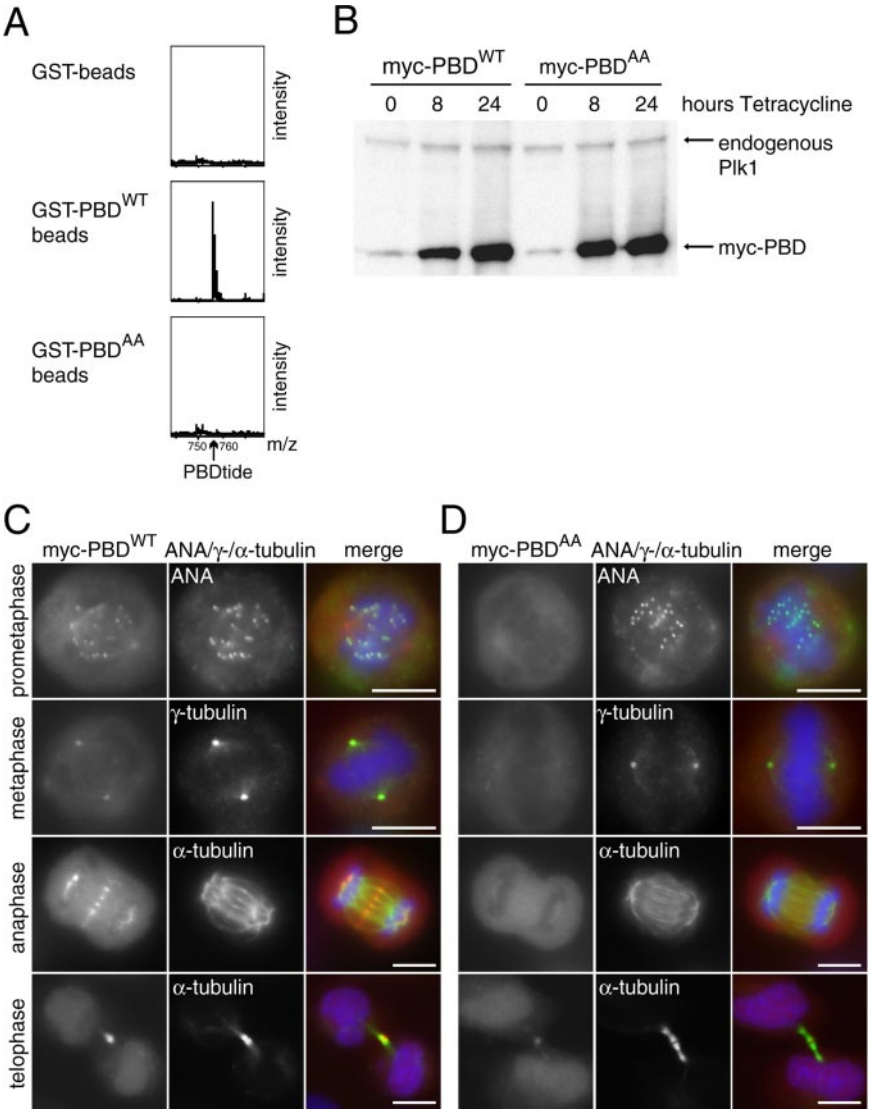

Figure 1. Localization of the Plk1 PBD to diverse spindle structures requires an intact phosphopeptide-binding motif. (A) In vitro analysis of phosphopeptide binding to GST-PBD^{WT}-, GST-PBD^{AA}-, and control (GST)-coated glutathione-Sepharose beads. Phosphopeptide binding was determined by MS. Only with GST-PBD^{WT}, a phosphopeptide (PBDtide) of the correct *m/z* ratio, was detected. (B) Expression analysis of Plk1 PBD^{WT} and PBD^{AA} in stable cell lines induced with tetracycline for the indicated time durations. Equal amounts of cell lysates were probed with anti-Plk1 antibody after Western blotting. Endogenous Plk1 and the expressed myc-tagged Plk1 PBDs are indicated. (C) Myc-PBD^{WT} and (D) myc-PBD^{AA} stable cell lines were induced for 8 h with tetracycline and then fixed and permeabilized with formaldehyde/Triton X-100, or −20°C methanol for γ-tubulin staining. Cells were analyzed by indirect immunofluorescence microscopy using anti-myc-tetramethylrhodamine B isothiocyanate (red); DAPI (blue); and either ANA autoimmune serum (green), anti-γ-tubulin (green), or anti-α-tubulin (green) antibodies to reveal colocalization with kinetochores, centrosomes, and spindle microtubules, respectively. Merged pictures are shown at the right. Bars, 10 μm.

resuspending them in fixation solution (3:1 methanol/acetic acid). The fixed cells were incubated at 4°C for at least 20 min, washed three more times with the fixation solution, and finally, 10 μl of each cell solution was dropped on a −20°C HCl-treated coverslip that had been moistened before by breathing on to it. After drying of the coverslip on a wet Kleenex tissue over a 60°C heating block, spreads were stained for 5 min with 0.4 μg/ml DAPI and mounted.

In Vitro Phosphopeptide Binding

Recombinant GST, GST-PBD^{WT}, and GST-PBD^{AA} were purified from *Escherichia coli* using glutathione-Sepharose beads (GE Healthcare, Little Chalfont, Buckinghamshire, United Kingdom). These immobilized recombinant proteins were incubated in HEPES binding buffer (25 mM HEPES, pH 7.4, 2 mM EGTA, 2 mM $MgCl_2$, 1 mM DTT, and 100 ng/ml okadaic acid) containing 75 μM of the optimal PBD-binding phosphopeptide (Elia *et al.*, 2003a). After overnight incubation at 4°C, the beads were washed three times with binding buffer, and bound peptides were subsequently eluted with 30% formic acid at room temperature. The presence of phosphopeptides in these eluates was then determined by matrix-assisted laser desorption ionization (MALDI) mass spectrometry (MS).

RESULTS

An Intact Phosphopeptide-binding Motif Is Required for Localization of the Plk1 PBD

To analyze the role of the Plk1 PBD in mitotic progression, stable tetracycline-inducible cell lines were generated to express myc-tagged PBD wild-type (PBD^{WT}) or a PBD mutant (PBD^{AA}) in which His538 and Lys540, two residues critical for phosphopeptide binding, were changed to alanine residues. To verify the inability of this mutant to bind to phosphorylated residues, glutathione *S*-transferase (GST)-tagged PBD^{WT} and PBD^{AA} were produced. In vitro binding studies with these immobilized proteins showed that PBD^{WT}, but not PBD^{AA}, readily interacted with the consensus PBD-binding phosphopeptide (PBDtide), as analyzed by mass spectrometry (Figure 1A), confirming finding of a previous study (Elia *et al.*, 2003b). The addition of tetracycline to the stable cell lines induced the expression of both myc-PBD^{WT} and myc-PBD^{AA}. After 24 h, the exogenous proteins reached ~10 times the level of endogenous Plk1, as quantified by Western blot analysis using a Plk1 antibody that recognizes the PBD (Figure 1B). Shorter induction times (8 h) yielded more moderate myc-PBD expression levels, better suited for the analysis of subcellular localization (Figure 1, B, C, and D). The myc-tagged PBD proteins were visualized by staining with anti-myc antibodies, and, simultaneously, the induced cells were costained with antibodies against γ-tubulin, α-tubulin, and ANA autoimmune serum, markers for centrosomes, microtubules, and kinetochores, respectively. The

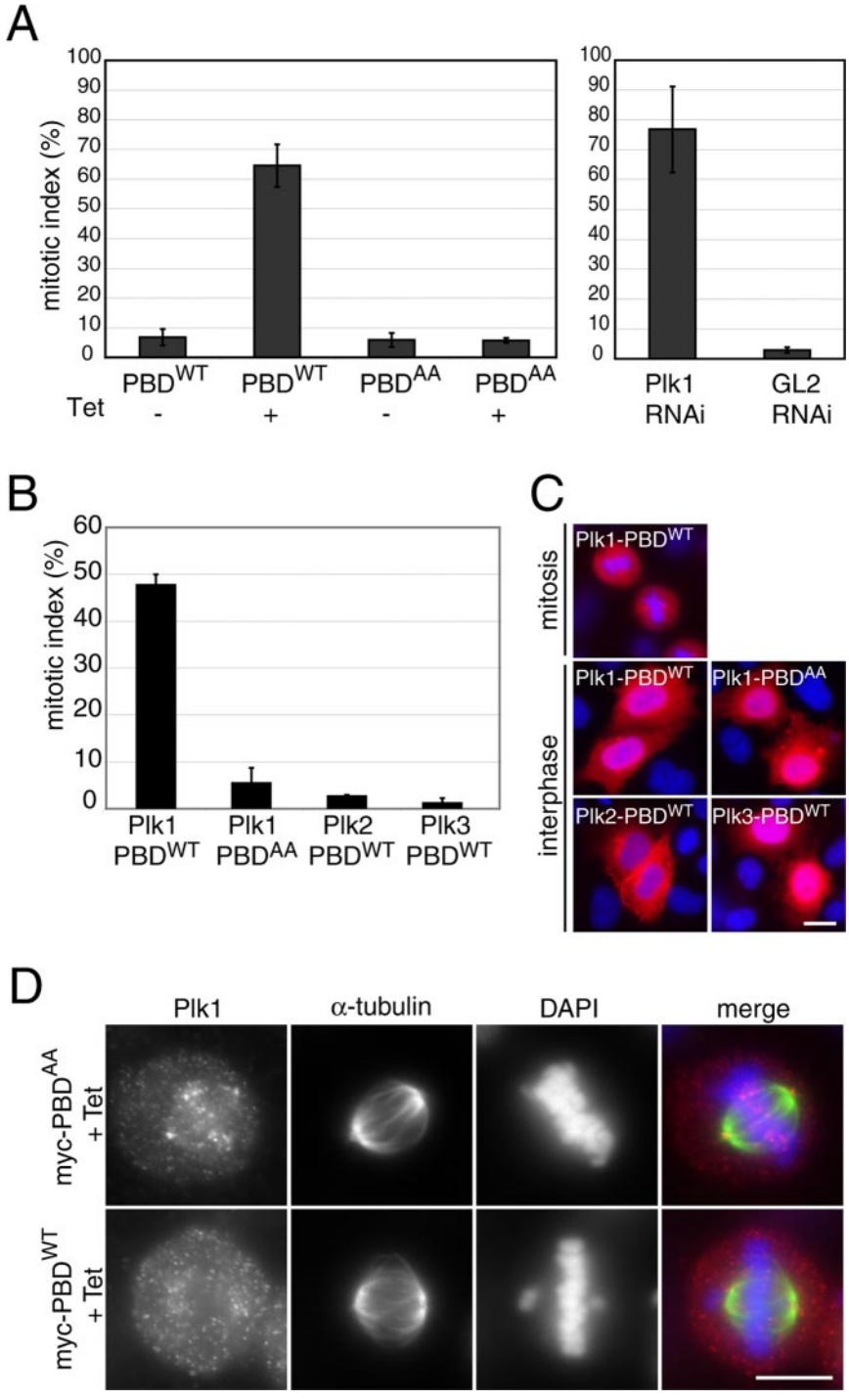

Figure 2. Overexpression of the Plk1 PBD^{WT} results in endogenous Plk1 displacement and mitotic arrest. (A) Mitotic indexes of PBD^{WT} and PBD^{AA} stable cell lines after treatment for 24 h with (Tet+) or without (Tet−) tetracycline (left graph). The mitotic indexes of cells treated for 36 h with Plk1 and control (GL2) siRNA duplexes are also shown (right graph). The mitotic indexes were determined by immunofluorescence microscopic analysis of the stained DNA. Histograms show results of three independent experiments (300–500 cells each), and bars indicate standard deviations. (B) Mitotic indexes of cells transiently transfected with myc-tagged PBD^{WT} and the PBD^{AA} mutant form of Plk1 as well as the wild-type PBDs of Plk2 and Plk3, respectively. After 48 h of transient transfection, cells were fixed and permeabilized with formaldehyde/Triton X-100 and stained with anti-myc antibody (9E10-tetramethylrhodamine B isothiocyanate) and DAPI. The mitotic indexes of the transfected (myc-positive) cells were then determined by immunofluorescence microscopic analysis of the stained DNA. Histograms show results of three independent experiments (>200 cells each), and bars indicate standard deviations. (C) Immunofluorescence images of cells expressing the indicated myc-tagged Plk-PBD constructs. Cells were treated as described in B. (D) PBD^{WT} and PBD^{AA} stable cell lines were induced for 24 h with tetracycline and subsequently fixed and permeabilized with formaldehyde/Triton X-100. Cells were then analyzed by indirect immunofluorescence microscopy using an anti-Plk1 N-terminal antibody (red), an anti-α-tubulin antibody (green) and DAPI (blue). Bars, 10 μm.

PBD^{WT} colocalized with kinetochores from prometa- to metaphase, with centrosomes from pro- to anaphase, and with the central spindle and the midbody during ana- and telophase (Figure 1C). This localization is virtually identical to that of endogenous Plk1 (Barr *et al*., 2004), confirming a critical role of the PBD in the subcellular distribution of Plk1 (Seong *et al*., 2002). In case of the PBD^{AA} mutant, no clear staining of either kinetochores or the central spindle could be observed in mitotic cells, and centrosome and midbody staining were clearly reduced (Figure 1D). These results suggest that Plk1 localization to the described structures is mediated largely via PBD-dependent docking to phosphorylated target proteins.

Overexpression of PBD^{WT} Results in Displacement of Endogenous Plk1 and Causes Mitotic Arrest

The short-term induction (8 h) of PBD expression described above did not significantly change the cell cycle profile, but longer induction times (24 h) resulted in a marked increase in the mitotic index in cell populations expressing PBD^{WT}, but not PBD^{AA} (Figure 2A, left). This increase in mitotic index was quantitatively similar to that observed after Plk1

depletion by appropriate siRNAs (Figure 2A, right), whereas treatment of cells with a control (GL2) siRNA produced no effect (Figure 2A). In transient transfection studies, PBD^{WT} also caused a mitotic arrest, whereas PBD^{AA} was without effect, confirming the results obtained with the inducible cell lines (Figure 2B). Transient transfection was also used to explore the consequences of overexpressing the PBDs of Plk2 or Plk3. Neither one of these PBDs produced a significant mitotic arrest (Figure 2B), despite similar levels of expression, as judged by immunofluorescence staining of the individual transfected cells (Figure 2C). This indicates that only the Plk1 PBD^{WT} is able to compete effectively with endogenous Plk1 protein for the binding to phosphorylated docking proteins, despite similar phosphopeptide-binding specificities of these PBDs in vitro (Elia *et al.*, 2003b). Therefore, additional sequences or structural motifs within the docking proteins might further define PBD-binding specificity in vivo.

To corroborate these results and confirm that the Plk1 PBD could displace endogenous Plk1 from its intracellular binding partners, the localization of endogenous Plk1 was examined by using an antibody directed against the N terminus of Plk1. After expression of PBD^{AA} for 24 h, endogenous Plk1 could readily be detected on centrosomes and kinetochores (Figure 2D, top), but after expression of PBD^{WT}, this localization was clearly lost and only diffuse staining could be observed (Figure 2D, bottom). Because cells expressing PBD^{WT} became arrested in a prometaphase state (see below), we were unable to demonstrate the displacement of endogenous Plk1 from the central spindle and midbody. However, considering that Plk1 localization to these structures depends on PBD-mediated binding to phosphorylated kinesin-6, MKlp2 (Neef *et al.*, 2003), it seems legitimate to assume that PBD^{WT} overexpression would most likely displace endogenous Plk1 also from the central spindle and midbody. Together, the above-mentioned results suggest that PBD^{WT} overexpression causes cells to arrest in mitosis because excess PBD displaces endogenous Plk1 from PBD-docking proteins and hence from its sites of action.

PBD^{WT} Expression Allows Bipolar Spindle Formation but Causes Chromosome Congression Defects

To better understand the physiological importance of Plk1 localization, the phenotype of the mitotically arrested cells produced by PBD^{WT} overexpression was compared with that observed upon siRNA-mediated depletion of Plk1. This comparison revealed striking differences (Figure 3). In response to Plk1 depletion, ~87% of the mitotic cells exhibited spindles with monopolar or abnormally small bipolar microtubule arrays, centrosomes near each other, and chromosomes in a rosette-like arrangement (Figure 3A). Occasionally, Plk1-depleted cells showed bipolar spindles of apparently normal sizes, but these most often had unfocused spindle poles; moreover, they lacked a centrosome at one pole and instead contained the unseparated centrosome pair on the opposing pole (Figure 3A, bottom row). In contrast to Plk1-depleted cells, ~82% of the mitotic cells induced to express PBD^{WT} showed bipolar spindle formation with properly separated centrosomes (Figure 3B). However, although spindles appeared to be near-normal in these cells, a clear metaphase plate was rarely observed and instead, variable numbers of chromosomes failed to congress (Figure 3B). In summary, whereas Plk1-depleted cells mostly displayed unseparated centrosomes, monoastral spindles, and chromosomes in a rosette-like arrangement, PBD^{WT}-expressing cells formed bipolar spindles, but arrested with chromosome congression defects.

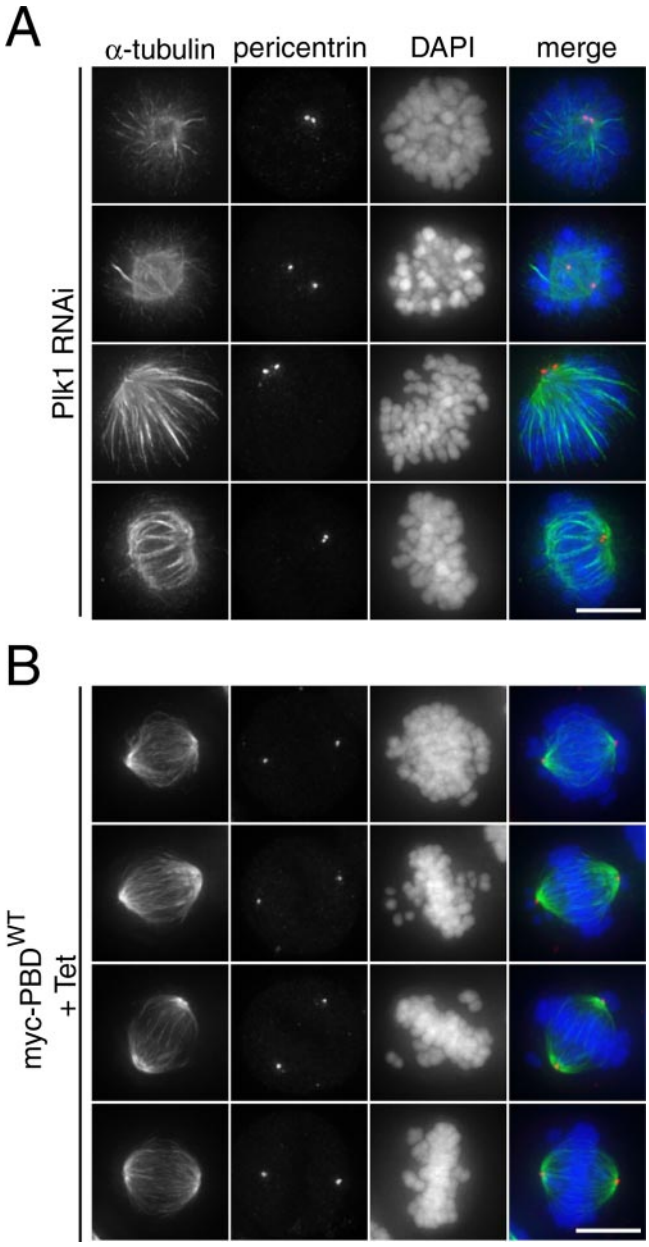

Figure 3. The mitotic phenotype of PBD^{WT}-expressing cells is distinct from the phenotype of Plk1-depleted cells. (A) HeLa S3 cells were treated with Plk1 siRNA duplexes for 36 h. After fixation and permeabilization, cells were analyzed by indirect immunofluorescence microscopy using anti-pericentrin (red), anti-α-tubulin (green) antibodies, and DAPI (blue) staining. (B) The myc-PBD^{WT} stable cell line was induced for 24 h with tetracycline. Cells were fixed, stained, and analyzed as described in A. Bars, 10 μm.

To further analyze the chromosome congression defect produced by PBD^{WT} overexpression, we next examined the kinetochore–microtubule attachments in these cells. In cells arrested by PBD^{WT} overexpression, the congressed chromosomes were clearly attached to kinetochore–microtubule bundles, termed kinetochore-fibers (K-fibers), whereas the uncongressed chromosomes did not show obvious K-fiber attachment (Figure 4A). The kinetochore-attached microtu-

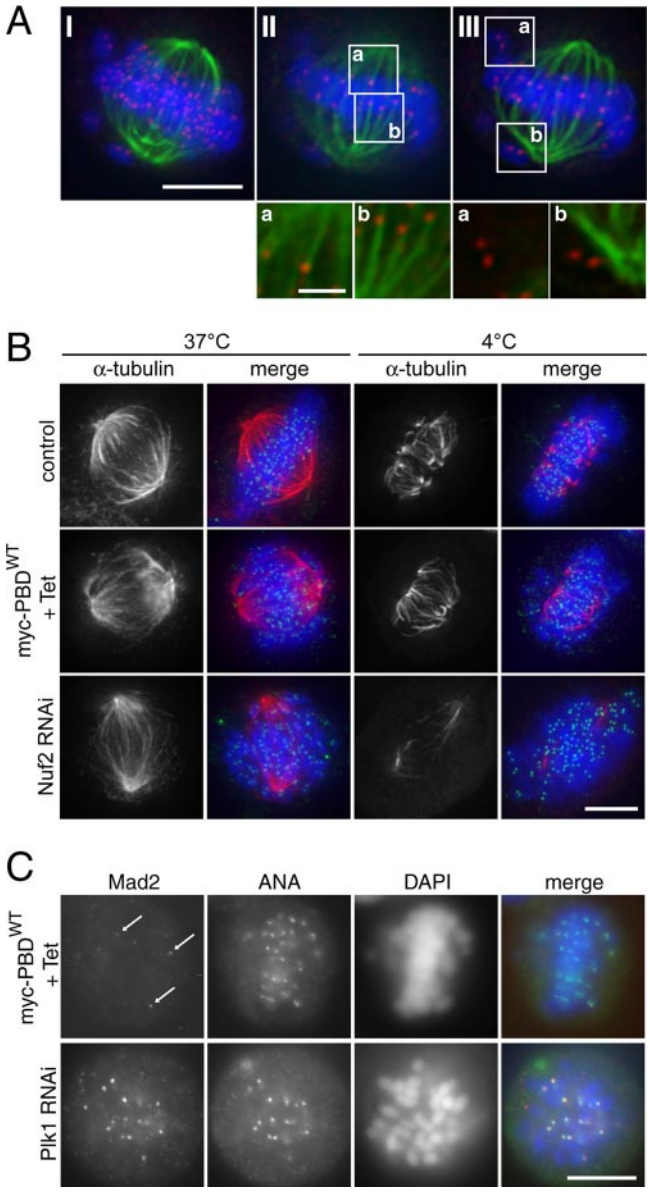

Figure 4. Lack of proper kinetochore–microtubule attachments on unaligned chromosomes in PBD^{WT}-expressing cells. (A) Myc-PBD^{WT} induced cells were fixed and permeabilized with formaldehyde/Triton X-100 and then stained with anti-α-tubulin (green), Hec1 (red), and DAPI (blue). A series of Z-stack images was taken from a mitotic cell and subsequently deconvolved. The left panel (I) shows a projection of the total Z-stack, whereas the middle (II) and right panels (III) show separate Z-stacks of the same cell (bar, 10 μm). Higher magnifications of the boxes indicated in II and III are presented below (bar, 5 μm). (B) The myc-PBD^{WT} stable cell line (middle row) was induced for 24 h with tetracycline and HeLa S3 cells (bottom panel) were treated with Nuf2 siRNA duplexes for 48 h. These cells, as well as control GL2-treated cells (top row), were then incubated for 10 min on ice followed by fixation and permeabilization with formaldehyde/Triton X-100. Cells were analyzed by indirect immunofluorescence microscopy using anti-α-tubulin antibody (red), CREST autoimmune serum (green), and DAPI (blue). (C) The myc-PBD^{WT} stable cell line (top row) was induced for 24 h with tetracycline, and HeLa S3 cells (bottom row) were treated with Plk1 siRNA duplexes for 36 h. After formaldehyde/Triton X-100 fixation, cells were analyzed by indirect immunofluorescence microscopy using anti-Mad2 antibody (red), ANA autoimmune serum (green), and DAPI (blue) staining. Arrows indicate Mad2 positive kinetochores at uncongressed chromosomes. Bars, 10 μm.

bules in PBD^{WT}-expressing cells were cold stable (Figure 4B), suggesting that proper kinetochore–microtubule attachments had occurred (Rieder, 1981). In contrast, kinetochore microtubules of cells depleted of the kinetochore protein Nuf2 were cold sensitive (Figure 4B), in agreement with previous results (DeLuca *et al*., 2002). In addition, in PBD^{WT}-expressing cells the attached kinetochores were under tension, as indicated by measurements of the interkinetochore distance, which was found to be 1.35 ± 0.27 μm, compared with 1.58 ± 0.44 μm in control cells. In contrast, kinetochores of uncongressed chromosomes showed interkinetochore distances of only 0.73 ± 0.14 μm, which is similar to the values for nocodazole-treated cells (0.72 ± 0.14 μm). This indicates that microtubule-dependent pulling forces could be generated in PBD^{WT}-expressing cells. In agreement with this conclusion, the spindle checkpoint protein Mad2, which is known to localize to kinetochores that lack proper microtubule attachment (Waters *et al*., 1998), could only be detected, at variable levels, at kinetochores of uncongressed chromosomes (Figure 4C). This is in striking contrast to Plk1-depleted cells in which most, if not all, kinetochores were strongly Mad2 positive, in agreement with previous results (Figure 4C) (Sumara *et al*., 2004). In both cases, though, the presence of Mad2 on at least some kinetochores points to spindle checkpoint activation (Howell *et al*., 2000; Shah and Cleveland, 2000). Indeed, the arrests induced by either Plk1 depletion or PBD^{WT} overexpression were spindle checkpoint dependent, because in both cases Mad2 depletion reduced the mitotic index by ~15-fold (our unpublished data), confirming and extending previous results (Seong *et al*., 2002; van Vugt *et al*., 2004b).

PBD Overexpression Does Not Interfere with Centrosome Maturation

One of the first demonstrated roles for Plk1 in mammalian cells relates to centrosome maturation during the G_2-to-M phase transition (Lane and Nigg, 1996). A hallmark of centrosome maturation is the recruitment of γ-tubulin ring complexes (γTuRC) to the centrosomes, which is required for increased microtubule nucleation at the onset of mitosis (Khodjakov and Rieder, 1999; Palazzo *et al*., 2000). We therefore analyzed and compared γ-tubulin recruitment in Plk1-depleted and PBD-overexpressing cells, using antibodies against centrin as a centriolar marker (Paoletti *et al*., 1996). In agreement with previous results, γ-tubulin recruitment was impaired in the absence of Plk1, but, interestingly, it was not significantly affected in cells expressing PBD^{WT} (Figure 5A). To further characterize this centrosome maturation defect, we also analyzed two other proteins, pericentrin and Aurora-A, which normally become enriched at mitotic centrosomes. Pericentrin was recruited to almost normal levels in both Plk1-depleted cells and PBD^{WT}-expressing cells, arguing that Plk1 depletion does not cause a general recruitment defect (Figure 5B). Moreover, because pericentrin is one of the proteins implicated in anchoring γTuRCs to mitotic centrosomes (Zimmerman *et al*., 2004), this also indicates that the loss of γ-tubulin is not caused by the absence of this anchoring protein.

Because Aurora-A kinase has also been implicated in centrosome maturation (Hannak *et al*., 2001; Berdnik and Knoblich, 2002), we also examined the fate of this protein. Remarkably, in Plk1-depleted cells Aurora-A no longer localized to centrosomes, as visualized by costaining with pericentrin, although it still localized to spindle microtubules surrounding the centrosomes (Figure 5C). In PBD-expressing cells, in contrast, Aurora-A localization to spindle poles was not affected (Figure 5C). Thus, Plk1 depletion

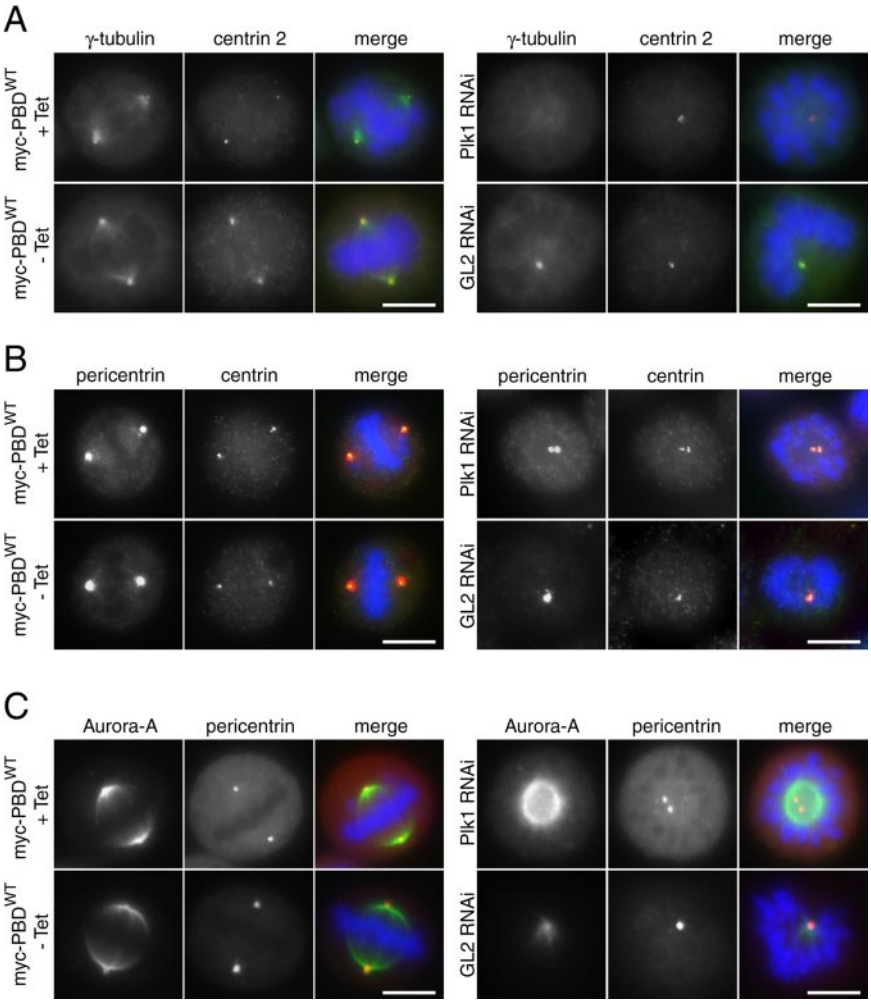

Figure 5. Centrosome maturation defects in Plk1-depleted but not PBD^{WT}-induced cells. (A) The myc-PBD^{WT} stable cell line (left) was induced (+Tet) for 24 h with tetracycline or left untreated (−Tet). HeLa S3 cells (right) were either treated with Plk1 or control (GL2) siRNA duplexes for 36 h. After −20°C methanol fixation, cells were analyzed by indirect immunofluorescence microscopy using anti-γ-tubulin (green), anti-centrin antibodies (red), and DAPI (blue) staining. (B) Same as in A, but cells were analyzed after anti-pericentrin (red), anti-centrin (green), and DAPI (blue) staining. (C) Same as in A, but cells were fixed and permeabilized with formaldehyde/Triton X-100 and analyzed after anti-Aurora-A (green) and anti-pericentrin (red), and DAPI (blue) staining. Bars, 10 μm.

impaired both the recruitment of γ-tubulin and Aurora-A to the centrosome, whereas PBD^{WT} overexpression did not detectably interfere with centrosome maturation. Together, these results show that both centrosome maturation and separation are defective in Plk1-depleted cells, but not in PBD^{WT}-overexpressing cells.

Chromatid Arm Separation Occurs in PBD-expressing Cells but Not in Plk1-depleted Cells

In vertebrate cells, Plk1 is required to remove the cohesin complex from sister chromatid arms during early mitosis (Sumara *et al*., 2002; Gimenez-Abian *et al*., 2004; Hauf *et al*., 2005). In agreement with this conclusion, the analysis of chromosome spreads showed that sister chromatid arms remained closely paired in Plk1-depleted cells, but not in nocodazole-arrested control cells (Figure 6). Interestingly, sister chromatid arms were also separated in cells expressing PBD^{WT} (Figure 6). This indicates that PBD overexpression, in contrast to Plk1 depletion, did not significantly interfere with the removal of the cohesin complex from chromosome arms.

The PBD Is Essential for Mitotic Progression

As shown above, the PBD-induced mitotic arrest phenotype most likely results from the displacement of endogenous Plk1 from its docking partners and sites of action (Figure 2D). The observation that, overall, the mitotic arrest phenotype produced by PBD overexpression was less severe than the Plk1 depletion phenotype suggested that not all Plk1 functions were dependent to similar extent on the correct localization of Plk1 activity. To test the hypothesis that some Plk1 functions strictly required correct localization of Plk1, whereas others could be performed even if Plk1 was displaced, we attempted to rescue the Plk1 depletion phenotype by different Plk1 constructs. These rescue experiments

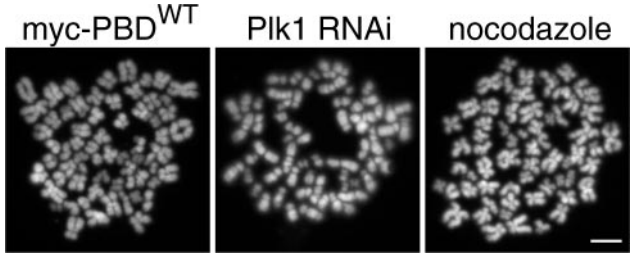

Figure 6. Chromosome spreads display dissociated chromosome arms in PBD^{WT}-induced but not Plk1-depleted cells. Mitotic myc-PBD^{WT} cells were obtained by tetracycline induction of the stable cell line for 24 h (left). HeLa S3 cells were either arrested in mitosis by siRNA-mediated Plk1 depletion (middle) for 36 h or by nocodazole treatment for 14 h (right). Mitotic chromosome spreads of all cells were stained with DAPI. Bar, 10 μm.

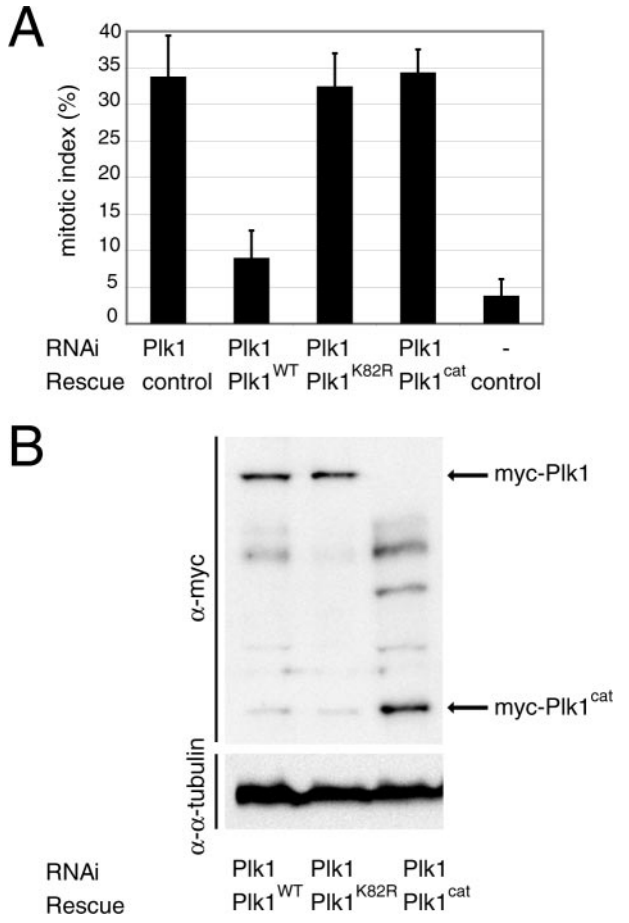

Figure 7. Expression of only the Plk1 catalytic domain in a Plk1-depleted background is not sufficient to overcome mitotic arrest. (A) HeLa S3 cells were cotransfected for 40 h with an empty RNAi vector (−) or an insert targeting Plk1, together with protein expression vectors (Rescue) coding for different myc-tagged Plk1 constructs or a myc-tagged control protein, as indicated. Cells were fixed and permeabilized with formaldehyde/Triton X-100 and were stained with anti-pericentrin antibody, anti-myc 9E10 antibody, and DAPI. The mitotic indexes were determined as in Figure 2B. Histogram shows the results of three independent experiments (300–500 cells each), and bars indicate standard deviations. (B) Expression levels of the different myc-tagged Plk1 proteins (Rescue) were analyzed by Western blotting using the anti-myc 9E10 antibody, and detection of α-tubulin was used as a loading control.

involved cotransfection of an RNAi vector targeting Plk1 with an RNAi-resistant expression plasmid coding for wild-type or mutant myc-tagged Plk1 proteins. Cotransfection of the Plk1 RNAi vector with a plasmid coding for a myc-tagged marker protein showed that ~34% of all transfected cells accumulated in mitosis (Figure 7A). Although less pronounced, this phenotype is similar to that observed after transfection of siRNA oligonucleotides (compare Figure 7A with Figure 2A). Concomitant expression of myc-tagged $Plk1^{WT}$ with the Plk1-specific RNAi vector drastically reduced the mitotic index, whereas a catalytically inactive form of Plk1 ($Plk1^{K82R}$) failed to rescue (Figure 7A). These results confirm that Plk1 activity is required for progression through mitosis. Most importantly, expression of the Plk1 catalytic domain ($Plk1^{cat}$) was not sufficient to override the mitotic arrest produced by the Plk1-specific RNAi vector (Figure 7A). Because all myc-tagged Plk1 proteins were expressed to similar levels (Figure 7B), these differences cannot be attributed to different expression levels. These results therefore clearly show that PBD-dependent targeting of Plk1 is critical for mitotic progression.

The PBD Is Dispensable for Centrosome Maturation and Separation, but Not for Chromosome Congression

To determine which, if any, of the defects apparent in the Plk1-depleted cells could be rescued by expression of delocalized $Plk1^{cat}$, we investigated the corresponding arrest phenotype in more detail. This analysis revealed that $Plk1^{cat}$ could indeed restore several of the Plk1-dependent processes that were defective in Plk1-depleted cells. Whereas proper centrosome separation and bipolar spindle formation were impaired in Plk1-depleted cells (Figure 8A; our unpublished data), in agreement with the data shown above (Figure 3A), these defects were no longer observed in depleted cells expressing the $Plk1^{cat}$ domain (Figure 8A). Moreover, both γ-tubulin and Aurora-A recruitment were clearly impaired in Plk1-depleted cells, but these defects could also be rescued by expressing the $Plk1^{cat}$ domain (Figure 8B). These experiments also confirmed that the catalytic domain alone is not able to localize to centrosomes and kinetochores, although some spindle-like staining could be observed (Figure 8, A and B). This is similar to the endogenous Plk1 localization in PBD^{WT}-expressing cells (Figure 2D) and suggests that Plk1 could interact in a PBD-independent manner with microtubules. The most straightforward interpretation of these data is that the PBD is essential for mitotic progression but not strictly required for centrosomal functions of Plk1.

Despite recovery from the centrosome and spindle formation defects, cells expressing the catalytic domain still arrested in mitosis, most likely because of chromosome congression defects (Figure 8, A and B). Quantitative analysis of the extent of chromosome congression revealed that in Plk1-depleted cells most chromosomes were not congressed, as expected for cells with monopolar spindles (Figure 8C, light gray bars). In depleted cells expressing the Plk1 catalytic domain, however, most cells showed partially congressed chromosomes, very similar to the phenotype seen with cells overexpressing the PBD (Figure 8C, dark gray and black bars, respectively). These results therefore indicate that proper chromosome alignment requires PBD dependent targeting of Plk1 activity.

DISCUSSION

Human Plk1 plays several different roles during mitotic progression, and it is thought that these functions require precise targeting of Plk1 to particular subcellular structures such as centrosomes and kinetochores (Barr *et al.*, 2004). The recent demonstration that the C-terminal PBD of Plk1 serves as a phosphopeptide-binding domain has led to an attractive model according to which the temporal and spatial control of Plk1 action involves PBD-mediated targeting of the kinase to phosphorylated docking proteins (Elia *et al.*, 2003a,b). Here, we have examined the importance of PBD-mediated localization for different mitotic functions of Plk1. Specifically, we have analyzed the consequences of overexpressing wild-type or mutant PBDs in HeLa S3 cells. We found that PBD^{WT}, but not PBD^{AA}, localized to all known sites of Plk1 action (centrosomes, kinetochores, and the spindle midzone). Moreover, prolonged expression of the PBD^{WT} caused a mitotic arrest, almost certainly because of the displacement of endogenous Plk1 from PBD-docking proteins and hence its sites of action. Most interestingly, this arrest

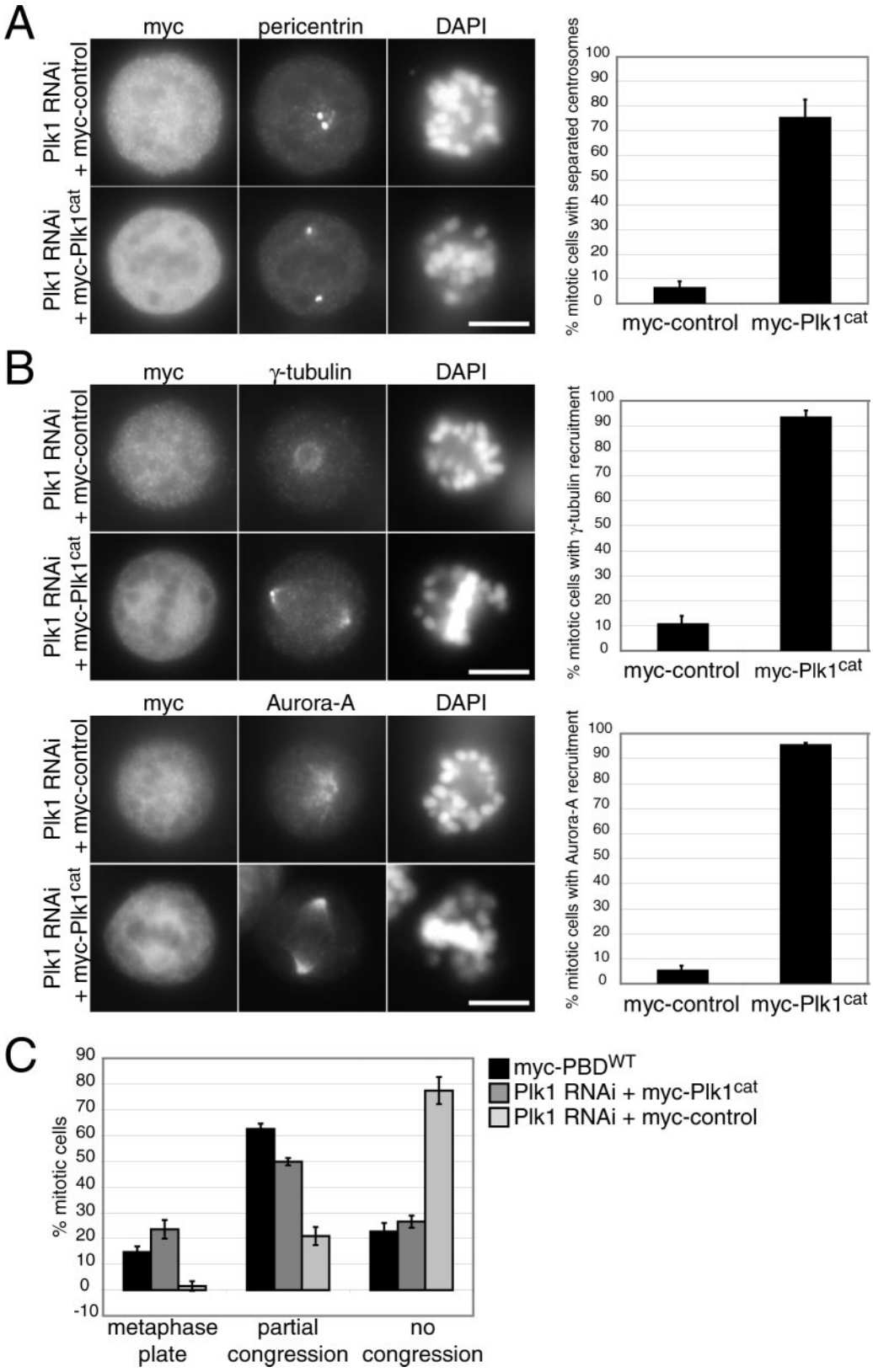

Figure 8. The PBD is dispensable for centrosome maturation and separation but required for chromosome congression. (A) HeLa S3 cells were cotransfected for 40 h with a Plk1-targeting RNAi vector and plasmids coding for either a myc-control protein or the myc-Plk1 catalytic domain. Cells were fixed and permeabilized with formaldehyde/Triton X-100 and then stained with anti-myc 9E10 antibody, DAPI, and anti-pericentrin antibody to visualize centrosome separation. Histogram shows the quantification of cells with separated centrosomes. Centrosomes were regarded as separated if they were positioned at opposite sites of the chromosome masses. Results are of three independent experiments (>100 cells each), and bars indicate standard deviations. (B) Same as in A, but cells were either fixed

Table 1. Comparison of the different mitotic defects

	Control	PBD^{WT}	Plk1 depletion	Plk1 depletion + catalytic domain
Centrosome maturation:				
γ-Tubulin recruitment	+	+	−	+
Aurora-A recruitment	+	+	−	+
Centrosome separation	+	+	−	+
Spindle formation	+	+	−	+
Chromosome congression	+	−	−	−
Loss of arm cohesion	+	+	−	Nd[a]

[a] Because of technical limitations, this defect could not be determined in these transiently transfected cells.

phenotype was clearly distinct from that seen in Plk1-depleted cells (Table 1). This suggests that proper Plk1 localization is critical for some, but not all, mitotic functions of Plk1. In support of this conclusion, we could demonstrate that overexpression of the Plk1 catalytic domain in a Plk1-depleted background resulted in a phenotype very similar to that seen in PBD-overexpressing cells (Table 1). This rescue experiment confirms that sufficient amounts of delocalized Plk1 activity can perform centrosome maturation, separation, and spindle formation, but not proper chromosome congression. From the perspective of therapeutic approaches aimed at inhibiting Plk1 activity, this observation opens the interesting possibility that drugs targeting the PBD could be tailored such as to interfere only with a subset of Plk1 functions.

Both PBD overexpression and Plk1 depletion resulted in a spindle checkpoint-dependent mitotic arrest, but the phenotypes of the arrested cells were strikingly different. In contrast to Plk1 depletion, PBD overexpression did not significantly impair centrosome maturation and separation, loss of sister chromatid arm cohesion, and bipolar spindle formation. Instead, PBD overexpression did interfere with chromosome congression. At first sight, one could argue that this defect might reflect direct inhibition of endogenous Plk1 by PBD. However, this interpretation is unlikely, for the following reasons. First, PBD overexpression was previously shown not to affect the bulk activity of endogenous Plk1 (Seong *et al*., 2002). Second, the critical chromosome congression defect was observed only in cells expressing PBD^{WT} but not in cells expressing a PBD^{AA} mutant. Considering that both wild-type and mutant PBDs are able to interact with the catalytic domain of Plk1 (Elia *et al*., 2003b), a direct inhibitory interaction of the PBD with endogenous Plk1 seems unlikely. Thus, the most straightforward interpretation of our results is that PBD^{WT}, but not PBD^{AA}, competes with endogenous Plk1 for the binding to phosphorylated docking proteins. This conclusion is strongly supported by our observation that endogenous Plk1 could be displaced from centrosomes and kinetochores by PBD^{WT} but not PBD^{AA}. Furthermore, our rescue experiments showed that Plk1-depleted cells expressing only the catalytic domain of Plk1 displayed a mitotic phenotype very similar to that seen in PBD^{WT}-overexpressing cells. Thus, although delocalized Plk1 activity seems to be sufficient for some Plk1 functions, it cannot provide all functions required for mitotic progression.

In agreement with previous results (Lane and Nigg, 1996; Sumara *et al*., 2004; van Vugt *et al*., 2004b), our study confirms that Plk1 is required for γ-tubulin recruitment during centrosome maturation. In addition, we discovered that the centrosomal recruitment of Aurora-A, a kinase also implicated in centrosome maturation and bipolar spindle formation (Nigg, 2001), was abolished in the absence of Plk1. In contrast, Aurora-A localization to spindle microtubules was not affected. These results clearly demonstrate that Plk1 regulates Aurora-A recruitment to the centrosome. Regardless of whether this Plk1 requirement reflects a direct or indirect mechanism, this observation suggests that Plk1 acts upstream of Aurora-A in centrosome maturation and spindle formation.

Because endogenous Plk1 prominently localizes to centrosomes, it may seem surprising that PBD-mediated displacement of Plk1 did not interfere with centrosome maturation and separation. It is difficult to rigorously exclude that very low levels of Plk1 might have remained at centrosomes in PBD^{WT}-expressing cells, and although undetectable by immunofluorescence microscopy, might have been sufficient to carry out the analyzed centrosome functions. However, the fact that overexpression of the catalytic domain in Plk1-depleted cells was sufficient to restore centrosome maturation and spindle assembly would argue that localized Plk1 activity is not absolutely required for the analyzed centrosome functions. In contrast, the catalytic domain alone was unable to restore sufficient chromosome congression to satisfy the spindle checkpoint, so that Plk1-depleted cells expressing only delocalized activity arrested with a phenotype closely resembling that seen in PBD-overexpressing cells. These results thus indicate that the investigated centrosomal functions of Plk1 are less dependent on localized Plk1 activity than the chromosome congression function.

Although suggested previously (Seong *et al*., 2002), a role of Plk1 in chromosome congression has not attracted attention, most likely because chromosome congression is diffi-

Figure 8 (facing page). and permeabilized with −20°C methanol and stained with anti-myc 9E10 antibody, anti-γ-tubulin antibody, and DAPI (top) or fixed and permeabilized with formaldehyde/Triton X-100 and stained with anti-myc 9E10 antibody, anti-Aurora-A antibody and DAPI (bottom). Histograms show the quantification of the recruitment of γ-tubulin and Aurora-A, respectively. Results are of three independent experiments (>50 cells each), and bars indicate standard deviations. (C). Histogram shows quantification of the different degrees of chromosome congression to the metaphase plate in PBD^{WT}-expressing cells (black bars), in cells expressing the Plk1 catalytic domain in a Plk1-depleted background (dark gray bars), and in Plk1-depleted cells (light gray bars). The term "partial congression" is used to describe cells in which a metaphase-like plate is present together with variable numbers of uncongressed chromosomes, whereas "no congression" describes cells that do not show an obvious metaphase plate. Results are of three independent experiments (100 cells each), and bars indicate standard deviations. Bars, 10 μm.

cult to study in Plk1-depleted cells, which arrest mostly with monoastral spindles. The exact nature of the chromosome congression defect in cells harboring only delocalized Plk1 activity remains to be determined, but our observation that nonaligned chromosomes were not attached to K-fibers in PBD-overexpressing cells suggests that microtubule capture or maintenance of kinetochore–microtubule attachments depends on localized Plk1 activity. Plk1 has long been known to localize to kinetochores (Arnaud *et al*., 1998), and with the identification of a PBD-dependent role of Plk1 in chromosome congression this strongly points to a critical function at this site. In future studies, it will thus be important to identify Plk1 PBD-interacting proteins among kinetochore components and to study their involvement in chromosome congression.

ACKNOWLEDGMENTS

We thank J. L. Salisbury for the monoclonal anti-centrin antibody, Roman Körner for MS analysis, and all our colleagues in the department, especially Francis Barr and Thomas Mayer, for helpful discussions. We also thank Francis Barr for critical reading of the manuscript. This study was supported by the Max Planck Society, the "Deutsche Forschungsgemeinschaft" (SFB646) and the "Fonds der Chemischen Industrie."

REFERENCES

Arnaud, L., Pines, J., and Nigg, E. A. (1998). GFP tagging reveals human Polo-like kinase 1 at the kinetochore/centromere region of mitotic chromosomes. Chromosoma *107*, 424–429.

Barr, F. A., Sillje, H. H., and Nigg, E. A. (2004). Polo-like kinases and the orchestration of cell division. Nat. Rev. Mol. Cell. Biol. *5*, 429–440.

Berdnik, D., and Knoblich, J. A. (2002). Drosophila Aurora-A is required for centrosome maturation and actin-dependent asymmetric protein localization during mitosis. Curr. Biol. *12*, 640–647.

Brummelkamp, T. R., Bernards, R., and Agami, R. (2002). A system for stable expression of short interfering RNAs in mammalian cells. Science *296*, 550–553.

Carmena, M., Riparbelli, M. G., Minestrini, G., Tavares, A. M., Adams, R., Callaini, G., and Glover, D. M. (1998). *Drosophila* polo kinase is required for cytokinesis. J. Cell Biol. *143*, 659–671.

Cheng, K. Y., Lowe, E. D., Sinclair, J., Nigg, E. A., and Johnson, L. N. (2003). The crystal structure of the human polo-like kinase-1 polo box domain and its phospho-peptide complex. EMBO J. *22*, 5757–5768.

DeLuca, J. G., Moree, B., Hickey, J. M., Kilmartin, J. V., and Salmon, E. D. (2002). hNuf2 inhibition blocks stable kinetochore-microtubule attachment and induces mitotic cell death in HeLa cells. J. Cell Biol. *159*, 549–555.

Descombes, P., and Nigg, E. A. (1998). The polo-like kinase Plx1 is required for M phase exit and destruction of mitotic regulators in *Xenopus* egg extracts. EMBO J. *17*, 1328–1335.

Eckerdt, F., Yuan, J., and Strebhardt, K. (2005). Polo-like kinases and oncogenesis. Oncogene *24*, 267–276.

Elbashir, S. M., Harborth, J., Lendeckel, W., Yalcin, A., Weber, K., and Tuschl, T. (2001). Duplexes of 21-nucleotide RNAs mediate RNA interference in cultured mammalian cells. Nature *411*, 494–498.

Elia, A. E., Cantley, L. C., and Yaffe, M. B. (2003a). Proteomic screen finds pSer/pThr-binding domain localizing Plk1 to mitotic substrates. Science *299*, 1228–1231.

Elia, A. E., Rellos, P., Haire, L. F., Chao, J. W., Ivins, F. J., Hoepker, K., Mohammad, D., Cantley, L. C., Smerdon, S. J., and Yaffe, M. B. (2003b). The molecular basis for phosphodependent substrate targeting and regulation of Plks by the Polo-box domain. Cell *115*, 83–95.

Gimenez-Abian, J. F., Sumara, I., Hirota, T., Hauf, S., Gerlich, D., de la, T. C., Ellenberg, J., and Peters, J. M. (2004). Regulation of sister chromatid cohesion between chromosome arms. Curr. Biol. *14*, 1187–1193.

Glover, D. M. (2005). Polo kinase and progression through M phase in *Drosophila*: a perspective from the spindle poles. Oncogene *24*, 230–237.

Golsteyn, R. M., Mundt, K. E., Fry, A. M., and Nigg, E. A. (1995). Cell cycle regulation of the activity and subcellular localization of Plk1, a human protein kinase implicated in mitotic spindle function. J. Cell Biol. *129*, 1617–1628.

Gumireddy, K., Reddy, M. V., Cosenza, S. C., Boominathan, R., Baker, S. J., Papathi, N., Jiang, J., Holland, J., and Reddy, E. P. (2005). ON01910, a non-ATP-competitive small molecule inhibitor of Plk1, is a potent anticancer agent. Cancer Cell *7*, 275–286.

Hannak, E., Kirkham, M., Hyman, A. A., and Oegema, K. (2001). Aurora-A kinase is required for centrosome maturation in *Caenorhabditis elegans*. J. Cell Biol. *155*, 1109–1116.

Hauf, S., Roitinger, E., Koch, B., Dittrich, C. M., Mechtler, K., and Peters, J. M. (2005). Dissociation of cohesin from chromosome arms and loss of arm cohesion during early mitosis depends on phosphorylation of SA2. PLoS Biol. *3*, e69.

Howell, B. J., Hoffman, D. B., Fang, G., Murray, A. W., and Salmon, E. D. (2000). Visualization of Mad2 dynamics at kinetochores, along spindle fibers, and at spindle poles in living cells. J. Cell Biol. *150*, 1233–1250.

Jang, Y. J., Lin, C. Y., Ma, S., and Erikson, R. L. (2002a). Functional studies on the role of the C-terminal domain of mammalian polo-like kinase. Proc. Natl. Acad. Sci. USA *99*, 1984–1989.

Jang, Y. J., Ma, S., Terada, Y., and Erikson, R. L. (2002b). Phosphorylation of threonine 210 and the role of serine 137 in the regulation of mammalian polo-like kinase. J. Biol. Chem. *277*, 44115–44120.

Khodjakov, A., and Rieder, C. L. (1999). The sudden recruitment of gamma-tubulin to the centrosome at the onset of mitosis and its dynamic exchange throughout the cell cycle, do not require microtubules. J. Cell Biol. *146*, 585–596.

Kraft, C., Herzog, F., Gieffers, C., Mechtler, K., Hagting, A., Pines, J., and Peters, J. M. (2003). Mitotic regulation of the human anaphase-promoting complex by phosphorylation. EMBO J. *22*, 6598–6609.

Lane, H. A., and Nigg, E. A. (1996). Antibody microinjection reveals an essential role for human polo-like kinase 1 (Plk1) in the functional maturation of mitotic centrosomes. J. Cell Biol. *135*, 1701–1713.

Lee, K. S., Park, J. E., Asano, S., and Park, C. J. (2005). Yeast polo-like kinases: functionally conserved multitask mitotic regulators. Oncogene *24*, 217–229.

Lee, K. S., Yuan, Y. L., Kuriyama, R., and Erikson, R. L. (1995). Plk is an M-phase-specific protein kinase and interacts with a kinesin-like protein, CHO1/MKLP-1. Mol. Cell. Biol. *15*, 7143–7151.

Lindon, C., and Pines, J. (2004). Ordered proteolysis in anaphase inactivates Plk1 to contribute to proper mitotic exit in human cells. J. Cell Biol. *164*, 233–241.

Liu, X., and Erikson, R. L. (2002). Activation of Cdc2/cyclin B and inhibition of centrosome amplification in cells depleted of Plk1 by siRNA. Proc. Natl. Acad. Sci. USA *99*, 8672–8676.

Lowery, D. M., Lim, D., and Yaffe, M. B. (2005). Structure and function of Polo-like kinases. Oncogene *24*, 248–259.

Martin-Lluesma, S., Stucke, V. M., and Nigg, E. A. (2002). Role of Hec1 in spindle checkpoint signaling and kinetochore recruitment of Mad1/Mad2. Science *297*, 2267–2270.

Mundt, K. E., Golsteyn, R. M., Lane, H. A., and Nigg, E. A. (1997). On the regulation and function of human polo-like kinase 1 (PLK1): effects of overexpression on cell cycle progression. Biochem. Biophys. Res. Commun. *239*, 377–385.

Neef, R., Preisinger, C., Sutcliffe, J., Kopajtich, R., Nigg, E. A., Mayer, T. U., and Barr, F. A. (2003). Phosphorylation of mitotic kinesin-like protein 2 by polo-like kinase 1 is required for cytokinesis. J. Cell Biol. *162*, 863–875.

Nigg, E. A. (2001). Mitotic kinases as regulators of cell division and its checkpoints. Nat. Rev. Mol. Cell. Biol. *2*, 21–32.

Palazzo, R. E., Vogel, J. M., Schnackenberg, B. J., Hull, D. R., and Wu, X. (2000). Centrosome maturation. Curr. Top. Dev. Biol. *49*, 449–470., 449–470.

Paoletti, A., Moudjou, M., Paintrand, M., Salisbury, J. L., and Bornens, M. (1996). Most of centrin in animal cells is not centrosome-associated and centrosomal centrin is confined to the distal lumen of centrioles. J. Cell Sci. *109*, 3089–3102.

Rieder, C. L. (1981). The structure of the cold-stable kinetochore fiber in metaphase PtK1 cells. Chromosoma *84*, 145–158.

Seong, Y. S., Kamijo, K., Lee, J. S., Fernandez, E., Kuriyama, R., Miki, T., and Lee, K. S. (2002). A spindle checkpoint arrest and a cytokinesis failure by the dominant-negative polo-box domain of Plk1 in U-2 OS cells. J. Biol. Chem. *277*, 32282–32293.

Shah, J. V., and Cleveland, D. W. (2000). Waiting for anaphase: Mad2 and the spindle assembly checkpoint. Cell *103*, 997–1000.

Smith, M. R., Wilson, M. L., Hamanaka, R., Chase, D., Kung, H., Longo, D. L., and Ferris, D.K. (1997). Malignant transformation of mammalian cells initi-

ated by constitutive expression of the polo-like kinase. Biochem. Biophys. Res. Commun. *234*, 397–405.

Smits, V. A., Klompmaker, R., Arnaud, L., Rijksen, G., Nigg, E. A., and Medema, R. H. (2000). Polo-like kinase-1 is a target of the DNA damage checkpoint. Nat. Cell Biol. *2*, 672–676.

Sumara, I., Gimenez-Abian, J. F., Gerlich, D., Hirota, T., Kraft, C., de la, T. C., Ellenberg, J., Peters, and J. M. (2004). Roles of polo-like kinase 1 in the assembly of functional mitotic spindles. Curr. Biol. *14*, 1712–1722.

Sumara, I., Vorlaufer, E., Stukenberg, P. T., Kelm, O., Redemann, N., Nigg, E. A., and Peters, J. M. (2002). The dissociation of cohesin from chromosomes in prophase is regulated by Polo-like kinase. Mol. Cell *9*, 515–525.

Takai, N., Hamanaka, R., Yoshimatsu, J., and Miyakawa, I. (2005). Polo-like kinases (Plks) and cancer. Oncogene *24*, 287–291.

Toczyski, D. P., Galgoczy, D. J., and Hartwell, L. H. (1997). CDC5 and CKII control adaptation to the yeast DNA damage checkpoint. Cell *90*, 1097–1106.

Vagnarelli, P., and Earnshaw, W. C. (2004). Chromosomal passengers: the four-dimensional regulation of mitotic events. Chromosoma *113*, 211–222.

van de Wetering, M., Oving, I., Muncan, V., Pon Fong, M. T., Brantjes, H., van Leenen, D., Holstege, F. C., Brummelkamp, T. R., Agami, R., and Clevers, H. (2003). Specific inhibition of gene expression using a stably integrated, inducible small-interfering-RNA vector. EMBO Rep. *4*, 609–615.

van Vugt, M. A., Bras, A., and Medema, R. H. (2004a). Polo-like kinase-1 controls recovery from a G2 DNA damage-induced arrest in mammalian cells. Mol. Cell *15*, 799–811.

van Vugt, M. A., van de Weerdt, B. C., Vader, G., Janssen, H., Calafat, J., Klompmaker, R., Wolthuis, R. M., and Medema, R. H. (2004b). Polo-like kinase-1 is required for bipolar spindle formation but is dispensable for anaphase promoting complex/Cdc20 activation and initiation of cytokinesis. J. Biol. Chem. *279*, 36841–36854.

Waters, J. C., Chen, R. H., Murray, A. W., and Salmon, E. D. (1998). Localization of Mad2 to kinetochores depends on microtubule attachment, not tension. J. Cell Biol. *141*, 1181–1191.

Zimmerman, W. C., Sillibourne, J., Rosa, J., and Doxsey, S. J. (2004). Mitosis-specific anchoring of gamma tubulin complexes by pericentrin controls spindle organization and mitotic entry. Mol. Biol. Cell *15*, 3642–3657.